Performance of an indigenous integrated slurry photocatalytic membrane reactor (PMR) on the removal of aqueous phenanthrene (PHE)

C. Nirmala Rani and S. Karthikeyan

ABSTRACT

In this study, a slurry photocatalytic membrane reactor (PMR) was developed and evaluated for the degradation of aqueous phenanthrene (PHE). During continuous process with a hydraulic retention time (HRT) of 140 min, the maximum PHE degradation and total organic carbon (TOC) removal efficiencies were found to be 97% and 79%, respectively. The reuse and recovery potential of TiO_2 was studied with continuous recycling. The major intermediates during photodegradation of PHE were found to be phenanthrenequinone, phenanthenol and fluorine. This study also includes an investigation of membrane fouling caused by hydrophilic nano TiO_2. The cake layer observed on the membrane surface was characterized by scanning electron microscopy (SEM), atomic force microscopy (AFM) and energy dispersive spectroscopy (EDS). In addition, the effect of operating parameters such as pH and permeate flux on membrane fouling were also investigated. Low permeate flux and alkaline conditions reduced membrane fouling.

Key words | membrane fouling, permeate flux, phenanthrene, photocatalytic membrane reactor, roughness

C. Nirmala Rani (corresponding author)
S. Karthikeyan
Centre for Environmental Studies,
Anna University,
Chennai 600025,
India
E-mail: *nirmalacrani@gmail.com*

INTRODUCTION

Polycyclic aromatic hydrocarbons (PAHs) are a class of hydrophobic organic compounds that are listed as top priority pollutants due to their carcinogenic, mutagenic and toxic properties. They are fused ring compounds with carbon and hydrogen atoms arranged either in linear or cluster structure and are resistant to biological degradation. PAHs are one of the persistent organic pollutants (POPs) (Rani & Karthikeyan 2016) which enter the environment through various anthropogenic sources such as oil spills, waste incineration, wood combustion, atmospheric deposition, coal gasification, vehicular exhausts and industrial discharges. Volcanic eruption and forest fires involve emission of dust and gases. As a consequence of emission, PAHs are released into the environment (Freeman & Cattell 1990; Xiao *et al.* 2014; Abdel-Shafy & Mansour 2016; Kozak *et al.* 2017) and hence both are the main sources of PAHs. The presence of PAHs in drinking water may be due to contaminated source water or from contamination in pipes coated with coal tar in the water supply system.

Water contaminated by PAHs can be treated in biological treatment plants by adsorption with activated carbon or other adsorbents (Vela *et al.* 2012). For higher concentration of pollutants, biological treatment seems to be uneconomical (Adewuyi 2005). Conventional methods such as coagulation (Moursy & Abdel-Shafy 1983) and chlorination (Harrison *et al.* 1976; Pereira *et al.* 2004) removed these compounds only to a limited extent. Moursy & Abdel-Shafy (1983) obtained the total PAHs removal of 32% during chemical coagulation using alum. Moreover, chlorination was limited due to the disinfection by products which have been linked to different types of cancers and adverse reproductive outcomes (Pereira *et al.* 2004). The moderate removal of these compounds in the above-mentioned methods led the researchers to focus their work on advanced oxidation processes (AOPs). AOPs were found to be very effective to remove toxic, non-biodegradable, recalcitrant organic micropollutants from water (Comninellis *et al.* 2008) by means of highly reactive hydroxyl radical $OH^{\bullet}$. These methods produce significant changes in the chemical structure of pollutants and are based on catalytic and photochemical processes. The end products of AOPs are eco-friendly and these processes can also make use of

doi: 10.2166/wst.2018.220

solar energy as a light source rather than artificial light sources which reduce the treatment cost (Muruganandham *et al.* 2014). Fenton's reagent or ozone is the most commonly studied chemical oxidation method for the removal of PAHs. Sofia *et al.* (2006) investigated the efficiencies of Fenton's reagent and ozone for PAHs degradation and reported that Fenton's reagent (40–86% degradation efficiency) was more effective than ozone (10–70% removal efficiency) due to its stronger oxidation conditions. Bavel (2006) reported that low molecular weight (LMW) PAHs were more susceptible to degradation than high molecular weight (HMW) PAHs. As a result of this, the relative abundance of (HMW) PAHs increased after chemical oxidation treatment, particularly after ozone treatment and reduced the degradation efficiency. The operating costs during ozonation were less than that required by conventional thermochemical methods such as wet air oxidation which requires high pressures and temperatures (Psillakis *et al.* 2004). Moreover, the cost of ultrasound treatment of contaminants was found to be higher compared to other AOPs (Mahamuni & Adewuyi 2010). Meanwhile, heterogeneous photocatalysis with TiO_2 had attracted many researchers and was found to successfully degrade organic pollutants (Anandan *et al.* 2007) due to various advantages viz. operation at room temperature, low pressure condition, high degradation efficiency, non-necessity of adding chemicals, effective reuse of catalyst and complete degradation and mineralization of compound molecules (Herrmann 1999).

During TiO_2 photocatalysis, when incident photons of wave length less than 385 nm are adsorbed by TiO_2, electrons are promoted from valence band to conduction band leaving positive holes in valence band. These holes are capable of oxidizing the organics that are adsorbed and also to produce $OH^{\bullet}$ from adsorbed water molecules for the series of oxidation reactions. However, the electrons and holes may recombine and reduce the photocatalytic efficiency of the process. During heterogeneous photocatalysis, the liquid phase organic compounds are degraded into its corresponding intermediates and further mineralized to simpler CO_2 and water (Chong *et al.* 2010). There are two types of photocatalytic reactors in general; slurry (photocatalyst in suspension) and immobilized (photocatalyst supported on a carrier material). Slurry reactors have the problem of separation of photocatalyst from the reaction mixture. In addition, slurry reactors are not economically and ecologically feasible options as long as they have adequate means to retain and recycle the photocatalyst within the treatment unit. This problem could be overcome in the immobilized reactors (Wang *et al.* 2009). However, immobilized reactors have certain drawbacks such as (i) reduction in surface area, (ii) durability of the catalyst, and (iii) increased operating costs (Erdei *et al.* 2008). On the other hand, if slurry photocatalytic reactor is coupled with membrane separation, it may resolve the problem of catalyst separation. In integrated photocatalytic-membrane reactor, membrane acts as a barrier to confine the catalyst within the system which increases the residence time of pollutants and hence favors simultaneous photodegradation and separation. The separation characteristics of the membrane help to maintain the required amount of TiO_2 in suspension. However, the deposition of TiO_2 fouling on the membrane surface severely affected the photocatalytic degradation efficiency, as well as filtration efficiency, of the membrane and this fouling was found to be profound during continuous filtration (Damodar *et al.* 2010; Jiang *et al.* 2010). The cake layer formed on the membrane surface was found to be the main mechanism responsible for fouling (Zhang *et al.* 2012). The severity of membrane fouling and reversibility of fouling depends on the zeta potential of the particles in the feed solution and the membrane surface and hence the membrane surface have significant impact either positive or negative on the filtration process (Moritz *et al.* 2001).

There are five types of configurations of PMRs experimented by various researchers. They are (i) slurry PMRs with microfiltration (MF)/ultrafiltration (UF) membranes with cross flow mode of filtration where the membrane module is kept separately from the photoreactor (Sarasidis *et al.* 2014), (ii) slurry PMRs with MF/UF membranes with cross flow mode of filtration where a flat sheet or hollow fibre membrane module is submerged in the photoreactor (Erdei *et al.* 2008; Damodar *et al.* 2010), (iii) PMR in which membrane module is submerged in the slurry with UV lamps surrounding the reactor (Fernandez *et al.* 2014), (iv) PMRs with TiO_2 doped membranes (Rahimpour *et al.* 2011), and (v) PMRs with membrane distillation system (Qu *et al.* 2014). Among all PMRs, submerged slurry PMRs where the membrane confines photocatalyst particles seems to be better solution for the removal of pharmaceuticals and endocrine disrupting compounds in aqueous solutions.

There are mainly two drawbacks in the existing PMRs: (i) non uniform irradiation (light source is placed outside/inside the photoreactor) and (ii) no simultaneous photodegradation and separation (membrane module is kept outside/on one side of the submerged photoreactor).

Taking these drawbacks into consideration, we have developed a slurry PMR which ensures uniform irradiation (since UV lamp is placed at the center of the reactor) and simultaneous photodegradation and membrane separation (UV lamp and membrane are in the same reactor vessel) to favor for complete degradation and mineralization. This particular PMR occupies less space and hence reduces the cost of installation. The absence of reject stream eliminates the subsequent treatment of waste generated. The non-necessity of adding oxidants reduces the treatment cost. Membrane fouling in this PMR is efficiently controlled by means of cross flow mode of filtration and aeration. This indigenous slurry PMR was evaluated for PHE removal and the operating parameters were optimized during batch process with continuous recycling. Membrane fouling was found to be the major issue in slurry PMRs during continuous study. To enhance the performance of PMR, the operational conditions that minimize membrane fouling should be considered. Therefore, this research was carried out to study the effect of pH and permeate flux on membrane fouling. In addition, the performance of PMR for long-term operations was also studied through continuous experiments. The identification of intermediates during photodegradation of PHE in PMR were also studied.

MATERIALS AND METHODS

Chemicals

Phenanthrene ($C_{14}H_{10}$, MW-178) and titanium oxide (Evonik Degussa P25, Germany TiO_2, 21 nm transmission electron microscopy (TEM) size, 70% anatase and 30% rutile with Brunauer–Emmett–Teller (BET) surface area 50 m^2/g and band gap 3.2 eV) were purchased from Sigma Aldrich. The organic solvents (dichloromethane, acetonitrile, hexane), hydrochloric acid (36.5–38.0% HCl) and sodium hydroxide (99% NaOH) were of HPLC grade and purchased from Merck. For total organic carbon (TOC) analysis, Merck double distilled water was used. Feed solution was prepared by adding the required concentrations of model compound in distilled water. Required pH was adjusted by 0.1 M NaOH and 0.1 M HCl.

Experimental setup

The schematic diagram of a laboratory scale slurry PMR developed is shown in Figure 1. The reactor of 2.1 L volume comprises of a low pressure Hg UV-C lamp (16 W, 254 nm) and a flat sheet polyethersulphone (PES) YMLY 3001 – Synder LY membrane (size 305 mm ×

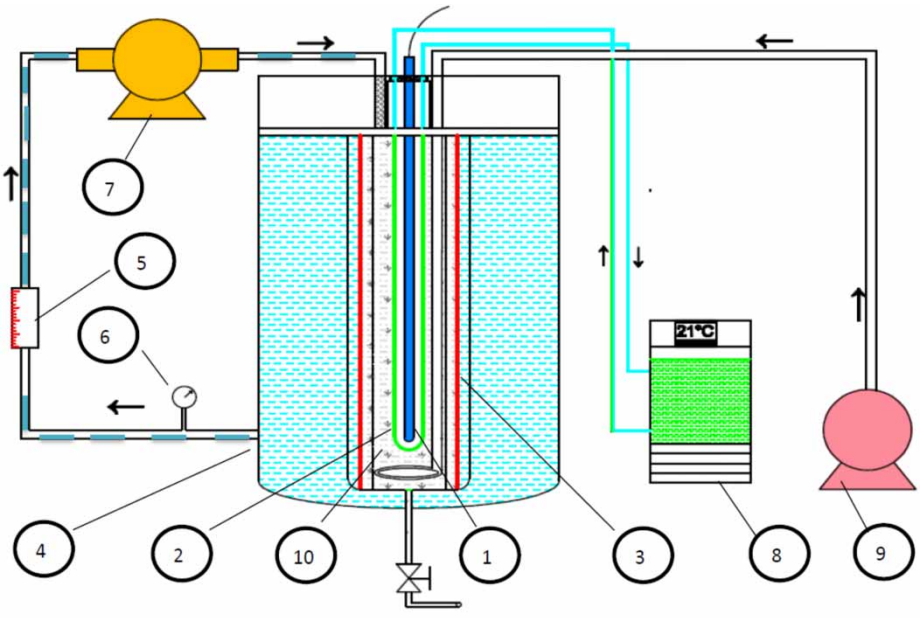

Figure 1 | Experimental setup of photocatalytic membrane reactor.

305 mm, MWCO 100 KDa, purchased from Sterlitech Corporation, Kent, WA, USA). The flat sheet membrane was rolled into a cylinder. In order to provide uniform irradiation, a UV lamp was placed at the center of the rolled membrane. The lamp which was in direct contact with the aqueous solution was protected by a double layered quartz glass tube through which water was recirculated. In order to collect the membrane permeate, the reactor was surrounded by an outer vessel made up of Plexiglas. An air diffuser plate was provided at the bottom of the reactor for which an air pump was connected. The physico-chemical properties of PHE and the characteristics of PES UF membrane are shown in Tables 1 and 2.

Analytical methods

The concentrations of PHE were quantified by gas chromatography (GC) mass spectroscopy (MS) using an Agilent Technology system comprising of a 6,890 GC fitted with a DB-5MS mid polar (5% phenyl 95% polydimethylsiloxane stationary phase) column of 30 m × 0.25 mm (inner dia) and helium carrier gas at 0.571 mL/min. Mass spectrometer (5,973) detection was used in electron impact mode and the ionization energy was set at 70 eV. The injection and interface temperature of the program were 280 °C. The temperature ramp was initially 40 °C for 1 min hold and for 10 °C, 300 °C for 5 min hold. The injection volume was 1 µL and the flow rate was 1.0 mL/min.

Liquid–liquid extraction (LLE) method was used to concentrate the sample. To extract the compound, 90 mL dichloromethane (DCM) was added to 30 mL of sample in a separating funnel, shaken well for 10 min and allowed to rest for 10 min. The organic extract was then allowed to pass through a funnel with sodium sulphate anhydride and was concentrated. These steps were repeated at least twice and the volume was concentrated to 5 mL DCM, evaporated and the final extract was analyzed by GC-MS. TOC was measured to determine the mineralization efficiency during photodegradation.

In this study, TOC of the samples were analyzed using TOC-VCPH/CPN PC-controlled TOC Analyzer (SHIMADZU Corporation, Kyoto, Japan) with an non-dispersive infra-red (NDIR) detector (680 °C combustion catalytic oxidation technique). Limit of detection (LOD) of the instrument was 4 µg/L and accuracy <2%. The repeatability of the measurements from GC-MS and TOC analyzer was checked by standard deviation (SD) and coefficient of variation (CV) and the error in measurement for all samples were estimated to be within ±5%. Intermediates were identified by NIST-11 library.

PHE degradation efficiencies were calculated using the formula:

$$\text{Degradation efficiency (\%)} = \frac{(C_{initial} - C_{final})}{C_{initial}} \times 100 \quad (1)$$

where $C_{initial}$ = Initial PHE concentration and
C_{final} = Final PHE concentration.

Characterization of the membrane

PES membranes have high rigidity and good chemical resistance due to their structures consisting of phenylene rings connected by sulfonyl (SO_2) groups. They have strong alkali resistance (Baker 2004). In this study, the morphology of the membrane surface and TiO_2 cake layer were examined using atomic force microscopy (AFM) and scanning electron microscopy (SEM) equipped with energy dispersive spectroscopy (EDS). To maintain the structure of the filtration cake, a sample after experimentation was taken from the flat sheet membrane, dried in ethanol and fixed in a polymer resin. Before analysis, the sample was cut to obtain the cross sections and sputtered with gold under vacuum. For AFM images and measurements, a silicon nitride ScanAsyst probe which utilizes the Peak Force Trapping Mechanism was used. The AFM membrane roughness (AFM-Ra) was calculated using the NanoScope Analysis software.

Table 1 | Physico-chemical properties of Phenanthrene

Compound	CAS number	Structure	Molecular formula	Molar mass	Water solubility at 25 °C	Log K_{ow}
Phenanthrene	85-01-8	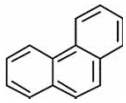	$C_{14}H_{10}$	178 g/mole	1.6 mg/L	4.46

Log K_{ow}, logarithm of octanol-water partition coefficient.

Table 2 | Characteristics of PES membrane

S. no.	Description	Specifications
1.	Manufacturer	Sterlitech Corporation, Kent, WA, USA
2.	Material	Polyethersulphone (PES)
3.	Module configuration	Flat sheet
4.	Module size	305 mm × 305 mm
5.	Filtration area	0.093025 m^2
6.	Filtration type	Ultrafiltration
7.	Hydrophilicity/ hydrophobicity	Hydrophobic
8.	Operational mode	Batch and continuous
9.	pH (recommended by the manufacturer)	2 to 11
10.	Molecular weight cut-off (MWCO)	100,000 Da
11.	Maximum flux	693–741 mL/min for 50 psi
12.	Roughness based upon AFM images	R_a(nm) = 1.131; R_q(nm) = 1.429; R_{sk} = −0.190; R_{ku} = 2.997

R_a, average roughness; R_q, root mean square roughness; R_{sk}, skewness; R_{ku}, kurtosis.

Fouling studies

To study TiO_2 fouling on membrane surface, batch studies were carried out with permeate recirculation. During this study, permeate was withdrawn at a constant flux of 31 L/m^2 h and recycled back to the tank. The concentration of TiO_2 was chosen to be 0.5 g/L. pH of the reaction solution was adjusted by 1 M HCl or 1 M NaOH. At every 30 min time interval, permeate turbidity and transmembrane pressure (TMP) were measured. Turbidity vs. concentrations curves were plotted from which the slurry TiO_2 concentrations were obtained. The effects of pH (5, 7 and 9) and permeate flux (20, 40 and 60 L/m^2 h or 31, 62 and 93 mL/min) on membrane fouling caused by TiO_2 deposition were evaluated. The experiments were carried out for 6 h at a constant flux condition.

Continuous studies

For continuous studies, experiments were conducted with the initial concentrations of PHE and TiO_2 as 1,000 mg/L and 0.5 g/L, respectively. Reaction mixture of 7 L volume was prepared in the feed tank and fed continuously to the reactor. In order to maintain a constant volume of the reaction mixture 2.1 L, the feed flow and the permeate rate were kept equal as 15 mL/min. The permeate flux and TMP were measured periodically. The membrane was cleaned when the pollutant removal efficiency dropped up to 5% from the previous test values. Each experiment was repeated at least twice in order to confirm the reproducibility of the results.

RESULTS AND DISCUSSION

Catalyst reuse and recovery

Batch studies were conducted to optimize the operating parameters such as PHE concentration, TiO_2 dosage and pH and the optimum values were found to be 1,000 µg/L, 0.5 g/L and 7, respectively. The photocatalytic ability of TiO_2 was evaluated by recycling the same slurry for seven cycles. Batch experiments were conducted in seven consecutive cycles with the same experimental conditions ([TiO_2] = 0.5 g/L, [PHE] = 1,000 µg/L, feed solution pH 7). Figure 2(a) and 2(b) show the PHE and TOC removal for seven cycles. During experimentation, it was observed that the PHE and TOC removal rates were greater when the catalyst was fresh. After the first cycle, the degradation and mineralization efficiencies reduced to a small extent and then remained constant for the next consecutive cycles. The reduction in PHE and TOC removals during these studies may be due to the deposition of suspended photocatalyst particles on the membrane surface and the reactor wall. However, obtained results revealed that the PMR system has a greater potential for long-term use and catalyst could be recycled and reused efficiently. Similar observations were made by others (Damodar & You 2010; Laohaprapanon *et al.* 2015). Damodar & You (2010) investigated the reusability of nano TiO_2 and reported that during continuous long-term operations, the membrane module was able to separate and recycle the catalyst efficiently within the reactor and the catalyst was also reused without much loss in degradation efficiency. Meanwhile, Laohaprapanon *et al.* (2015) investigated the reusability of ZnO and found that the photocatalytic activity of ZnO slightly dropped after the third cycle and the overall removal efficiency of RB5 decreased to 89% after the fifth cycle which was due to small corrosion of ZnO observed during experiment.

Continuous flow experiments

To appropriately design the main experiments and minimize the errors due to non-photocatalytic phenomena (adsorption), dark control tests were carried out. The

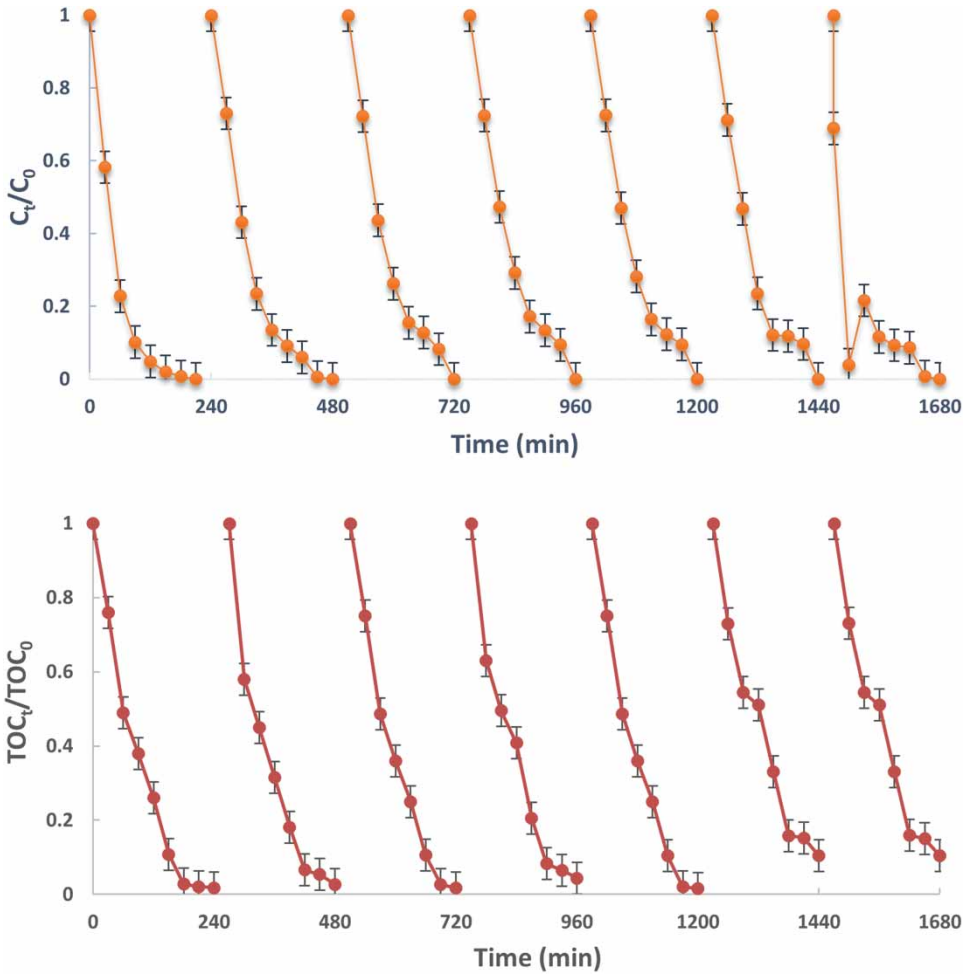

Figure 2 | Performance of PMR on (a) PHE removal and (b) TOC removal during seven cycles of catalyst reuse ([PHE] = 1,000 µg/L, [TiO_2] = 0.5 g/L, pH = 7, n = number of cycles). The error bars denote standard deviation.

adsorption of PHE molecules on the TiO_2 surface (in the absence of UV-C light) was evaluated to be 8%. The continuous mode PMR was operated after optimizing the operating parameters for photodegradation during batch mode. The reaction mixture containing 1,000 µg/L PHE and 0.5 g/L TiO_2 was continuously fed to the reactor with an HRT of 140 min. Figure 3 shows the performance of slurry PMR for PHE and TOC removal. The maximum PHE and COD removals obtained during experiments were 97% and 79%, respectively. The decrease in removal efficiencies may be due to the accumulation and deposition of TiO_2 particles on the reactor wall during membrane filtration which in turn reduces the availability of TiO_2 particles for photodegradation. After 140 min, the removal efficiencies remained constant. The reduction in removal efficiencies were not noticed. The aeration provided at a flow rate of 1.5 L/min should have prevented the deposition of TiO_2 particles on the membrane surface. A permeate flux of 20 L/m^2 h was maintained constant throughout the experimental run. Furthermore, the TOC of permeate was measured and was found to be 127 µg/L which confirm the presence of organics. By increasing the reaction time, complete degradation could be obtained (Nashio *et al.* 2006; Laohaprapanon *et al.* 2015). The results obtained in this study were consistent with the report of Damodar *et al.* (2010) who investigated the long-term operability of a slurry PMR ([RB5] = 75 to 225 mg/L, [TiO_2] = 0.5 g/L, HRT = 4 h). During this study, the authors found nearly 82–100% color and 45–93% TOC removals from the reactor. Laohaprapanon *et al.* (2015) evaluated the effectiveness of a continuous slurry PMR ([RB5] = 75 mg/L, [ZnO] = 1.25 g/L, HRT = 4 h) and reported that more than 95% color and 50–80% COD removals could be obtained from the reactor.

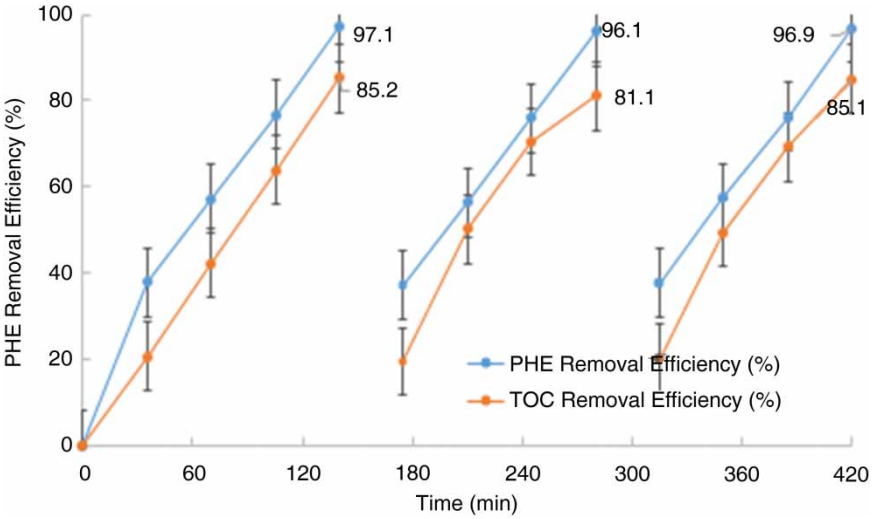

Figure 3 | Performance of slurry PMR in continuous mode ([PHE] = 1,000 µg/L, TiO_2. = 0.5 g/L). The error bars denote standard deviation.

Identification of intermediates

Since PMR enhances photodegradation, due consideration should be given to identify the intermediates that are formed during photocatalytic oxidation (PCO). The toxicity of these intermediates may be higher than the parent compound. The primary oxidizing species in heterogeneous photocatalysis are $OH^{\cdot}$ and $O_2^{\cdot}$. the chromatogram for the intermediates detected during PCO of phenanthrene degradation with irradiation time in the PMR is shown in Figure 4. To identify the intermediates, a sample of 30 mL was collected after 30 min from the reactor and was extracted by LLE and was analyzed on the same day. The intermediate compounds identified are given in Table 3. The common intermediates found during PCO were alcohol, ketone and quinone (Woo *et al.* 2009). Since the smaller molecules of intermediates were formed after many oxidation steps and some of them were short lived, they were not detected by GC-MS. The NIST 11 MS Library was used for intermediates identification. The library matched compounds, exhibited a degree of match better than 90% and the scan range was from m/z 40 to m/z 400 at 2.08 scans/s.

Reactive sites of PAHs

On PAHs, Dewar's activity number N_u is a measure of reactivity which reflects the localized energy and hence reactivity at a particular position (Dewar 1952). The smaller N_u value requires less destabilization energy and results in more reactive sites and hence higher reactivity. The N_u values of various positions of phenanthrene structure are shown in Table 1. The N_u values of positions 9 and 10 for PHE are comparatively lower than that of the other positions and hence the reactions mainly occur at these positions (Woo *et al.* 2009). The reason may be the attack of reactive species resulted for the better arrangement of electrons over the aromatic rings and the modified form became more stable (Lloyd 1989). The intermediate 9,10-phenanthrenequinone was identified by many researchers (Lin & Valsaraj 2003; Woo *et al.* 2009). The attack of $OH^{\cdot}$ on the ninth position of PHE would have resulted in the formation of 9,10-phenanthrenequinone. It is also a well-known intermediate in the conventional UV photolysis of PHE in natural water (Zeng *et al.* 2000). 9,10-phenanthrenequinone undergoes ring opening and reacts with alkyl radicals to form benzene dicarboxylic acid. The other intermediates were formed by further attack of hydroxyl radical on ninth position. Similar intermediate compounds were also detected by many others (Wen *et al.* 2002; Lin & Valsaraj 2003; Woo *et al.* 2009).

Membrane fouling in PMR

Membrane fouling is a major issue in slurry PMRs. It may increase the energy demand and hence increase in the operation costs and shorter life for the membrane. Hence, while designing PMRs, effective and efficient methods have to be applied to control and minimize fouling. In UF membrane concentration, polarization is a problem which occurs during the filtration of low molecular weight solutes or macromolecules. During membrane filtration, the rejected solutes diffuse slowly back to the bulk solution and create a concentration gradient above the membrane surface.

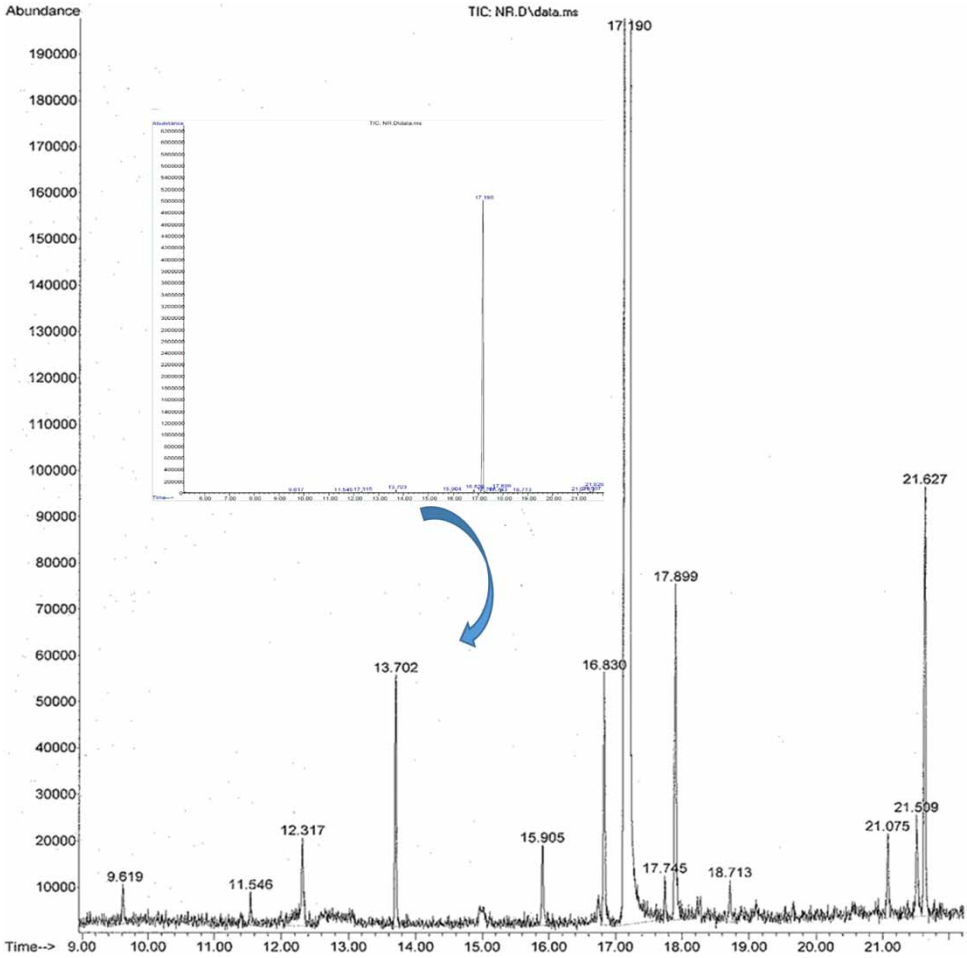

Figure 4 | GC-MS full scan mode chromatogram of LLE extract of the permeate sample collected after 30 min of operation.

The concentration of these molecules may react even 20–50 times higher than that of bulk solution (Baker 2004) and develop an osmatic back pressure that reduces the TMP of the system. The reduction in permeate flux in PMRs with UF membranes is due to concentration polarization and due to the deposition of materials present in feed solution on either side of the membrane or inside its pore structure (D'Souza & Mawson 2005).

AFM and SEM with EDS investigations of membrane and cake layer

The two and three dimensional surface AFM images of clean and used membranes at a scan size of 5 μm × 5 μm is shown in Figure 5. The brightest area represents the highest point on the membrane surface and the dark region indicates the membrane pores. These AFM images clearly indicate that the surface morphologies were altered by the deposition of TiO_2 nanoparticles on the membrane surface. The comparison of roughness parameters based on AFM images are given in Table 4.

The studies on TiO_2 fouling in PMRs found in the literatures explained the nature and mechanism of fouling using microscopic techniques, especially SEM, laser scanning microscopy (LSM) and TEM (Zhang *et al.* 2012; Mozia *et al.* 2014). The change in membrane topography was detected by AFM and AFM analysis of filtration cake layer revealed that the roughness of the membrane surface covered with TiO_2 layer was higher compared to that of clean membrane. The average roughness of the surface of the used membrane sample (28.041 nm) was higher than that of the clean membrane (1.131 nm). This may be due to the higher deposition of TiO_2 cake layer on the membrane surface. Similar results were observed by Mozia *et al.* (2014) in which the average roughness of the used UF membrane was found to be 22.8 nm while the roughness of the clean membrane was 1.5 nm.

Table 3 | Identification of degradation products generated during the photocatalytic membrane treatment of PHE: chemical structures with previous references

Compound/Reference	Retention time (min)	Molecular weight (g/mol)	Formula	Chemical structure
Phenanthrene (Lin & Valsaraj 2003; Woo *et al.* 2009)	17.190	178.234	$C_{14}H_{10}$	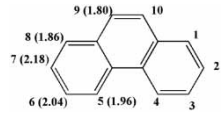
1,2-Benzene dicarboxylic acid (Phthalic acid) (Wen *et al.* 2002; Lin & Valsaraj 2003)	17.745	166.14	$C_8H_6O_2$	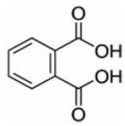
9,10-Phenanthrenequinone (Lin & Valsaraj 2003; Woo *et al.* 2009)	12.317	208.2	$C_{14}H_8O$	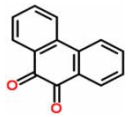
1,2-Benzene dicarboxylic acid, diisooctyl ester (Lin & Valsaraj 2003)	21.627	390.56	$C_{24}H_{38}O_4$	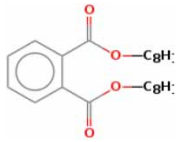
9H-Fluorene (Lin & Valsaraj 2003)	17.899	166.22	$C_{13}H_{10}$	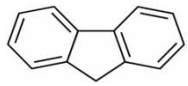
Dibutyl phthalate (Wen *et al.* 2002)	18.713	278.344	$C_{16}H_{22}$	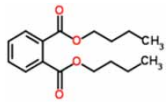
Phenanthrene, 2 methyl	15.905	192.261	$C_{15}H_{12}$	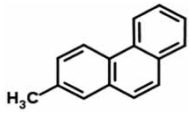
Phenanthrenol (Lin & Valsaraj 2003; Woo *et al.* 2009)	13.702	194.23	$C_{14}H_{10}O$	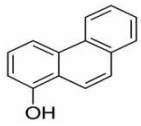
Bis 2-ethylhexyl phthalate (Wen *et al.* 2002; Lin & Valsaraj 2003)	21.075	390.56	$C_{24}H_{38}O_4$	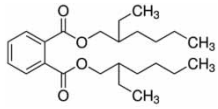

1, 2, 3, 4, 5, 6, 7, 8, 9 and 1.96, 2.04, 2.18, 1.86 in the chemical structure of phenanthrene indicate numbering and N_u (Dewar) values of PHE.

The micro-morphology of the fouled membrane and deposited cake layer was analyzed using X-ray EDS (GENESIS 4000, EDAX, USA) and the radial distribution of TiO_2 particles in the membrane surface was determined.

The fouling mechanisms can be of four types: (a) complete pore blocking by particle deposition, (b) intermediate pore blocking in which pores are clogged partially and cake grew on the deposited particle, (c) standard blocking in which membrane pores are narrowed due to adsorption of small particle on the wall of pores, and (d) cake filtration in which particles deposited on the membrane surface formed a cake layer and adds filtration resistance (Zhang *et al.* 2012). Figure 6(a) and 6(b) represent the cross section SEM images of clean and fouled membrane. A visual comparison of cake layer could be made. The TiO_2 particles entered into membrane pores should have formed a dense cake layer on the membrane surface. The presence of hydrophilic TiO_2 particles uniformly distributed on the membrane surface reduced the permeability of the membrane. Meanwhile, the reduction of permeate flux noticed during

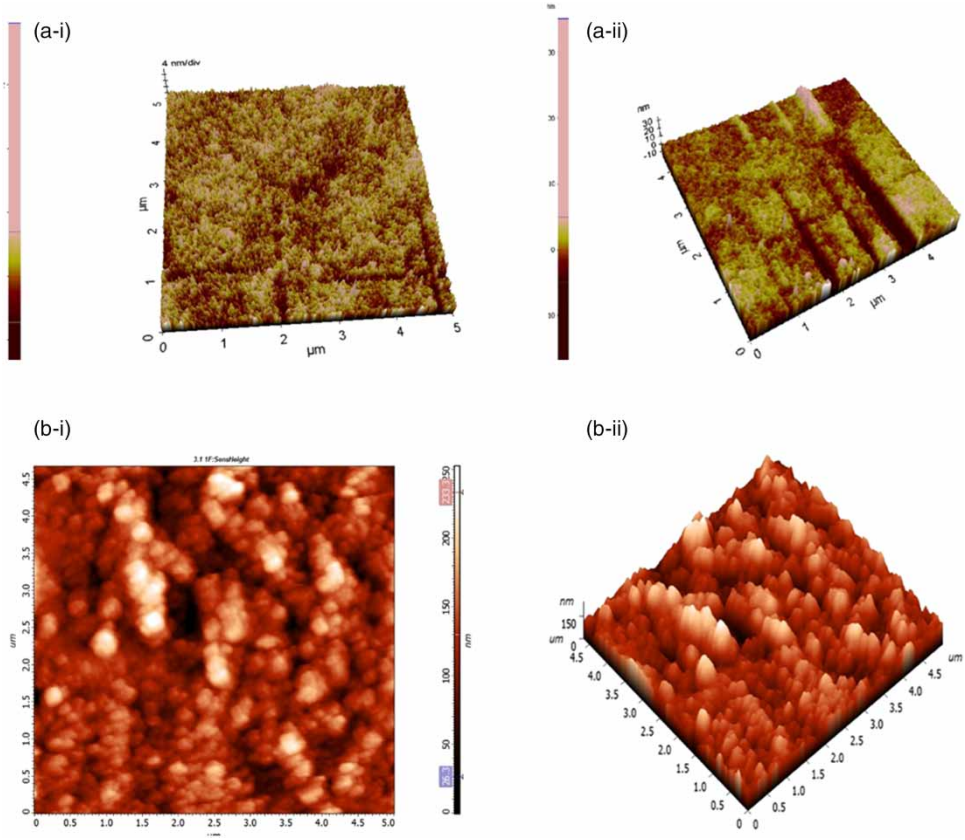

Figure 5 | AFM images of (a) clean (i) two dimensional image, (ii) three dimensional image and (b) used membrane (i) two dimensional image, (ii) three dimensional image.

Table 4 | The comparison of roughness coefficients

Membrane	Average roughness (R_a)	Root mean square roughness (R_q)	Skewness (R_{sk})
Clean membrane	1.131 nm	1.429 nm	0.190 nm
Used membrane	28.041 nm	34.242 nm	0.2845 nm

experimentation from 20 L/m^2 h to 8 L/m^2 h indicated the blockage of pores due to TiO_2 particles.

EDS analysis was carried out to investigate the distribution of TiO_2 nanoparticles on the membrane structure. Figure 6(c) illustrates the EDS spectra of used membrane. It can be seen that fouled PES membrane has a peak for titanium (Ti) which confirms the presence of Ti elements on the membrane surface. The white particles seen are the homogeneously dispersed TiO_2 nanoparticles on the membrane (Rahimpour *et al.* 2011).

The SEM-EDS results show that TiO_2 particles entered into the pores of PES membrane. Repeated backwashing could not recover these TiO_2 particles completely because of the strong affinity of nanosized TiO_2 particles towards the membrane surface. Instead, it could remove many parts of cake layer which results in partial removal of TiO_2 particles.

Effect of pH on fouling

In slurry PMRs, fouling is caused mainly by the deposition of photocatalyst particles on the membrane surface and could be measured in terms of turbidity of the reaction solution (tank turbidity) and TMP variation. The results are graphically represented in Figure 7(a) and 7(b). In PMR, batch recirculation mode experiments were carried out at a constant flux of 20 L/m^2 h. Permeate was withdrawn at a flow rate of 31 mL/min and recirculated back to the reactor. The decrease in turbidity represent the amount of TiO_2 fouled.

The effect of pH on membrane fouling could be explained with respect to (i) photodegradation of organic pollutants, (ii) adsorption of PHE on to TiO_2 particles, and (iii) interaction between TiO_2 particles and membrane. The possible explanation with respect to photodegradation

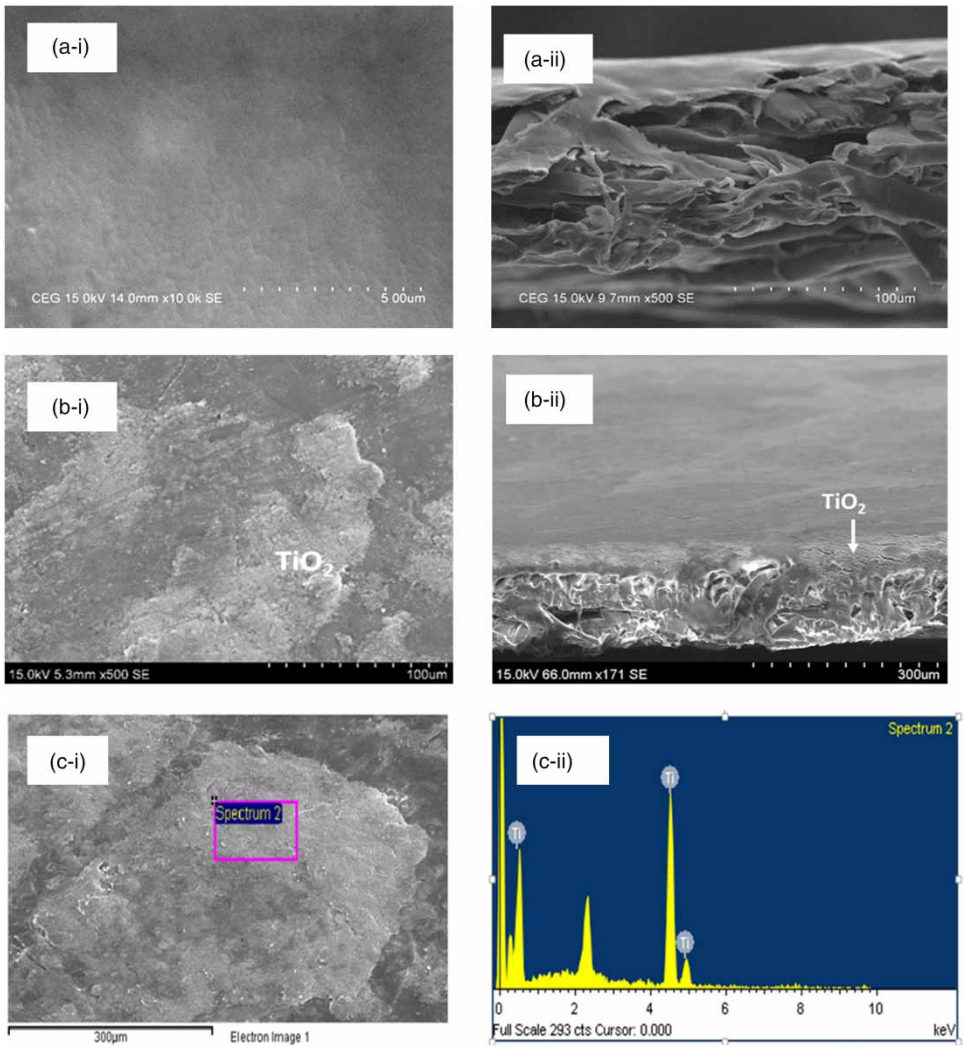

Figure 6 | SEM images of the (a) clean (i) top view and (ii) cross sectional view, (b) used membrane (i) top view and (ii) cross sectional view and (c) (i) and (ii) SEM with EDS image.

may be during photodegradation under acidic conditions, TiO_2 particles agglomerates and its particle size increases which in turn reduces the effective surface area for photons and reduces the photodegradation rate (Paz 2006). The explanation with respect to adsorption could be based upon the isoelectric point (P_{zc}) of TiO_2. During basic conditions ($pH > P_{zc}$), compound molecules with positive charges are adsorbed onto TiO_2 particles since TiO_2 surface is negatively charged. In contrast, during acidic conditions ($pH < P_{zc}$), TiO_2 surface is positively charged and hence compound molecules with negative charge are adsorbed. Since most of the organic pollutants are negatively charged (Mozia 2010), adsorption of more anionic PHE molecules onto TiO_2 is facilitated at acidic pH and hence adsorption behavior could be controlled using suitable pH. The explanation in terms of interaction between TiO_2 particles and the membrane surface could be during alkaline pH, there is improvement in membrane charge and hydrophilicity and, hence, reduction in concentration polarization and membrane fouling (Damodar *et al.* 2012; Zhang *et al.* 2015).

At acidic pH ($pH < 7$), the turbidity of the tank decreased with time due to the deposition of TiO_2 particles. However, at $pH = 7$, turbidity reduction was low and remained constant. This could be explained in terms of zeta potential (surface charge) and hydrophilicity of both membrane and TiO_2. The PES membrane was hydrophobic while TiO_2 particles are hydrophilic in nature and in the presence of UV light and water, due to the generation of hydroxyl radicals, its hydrophilicity increases. The deposition of these hydrophilic TiO_2 particles might have altered the hydrophilicity of the membrane. Furthermore, at $pH = 5$, there were no significant changes in TMP and it

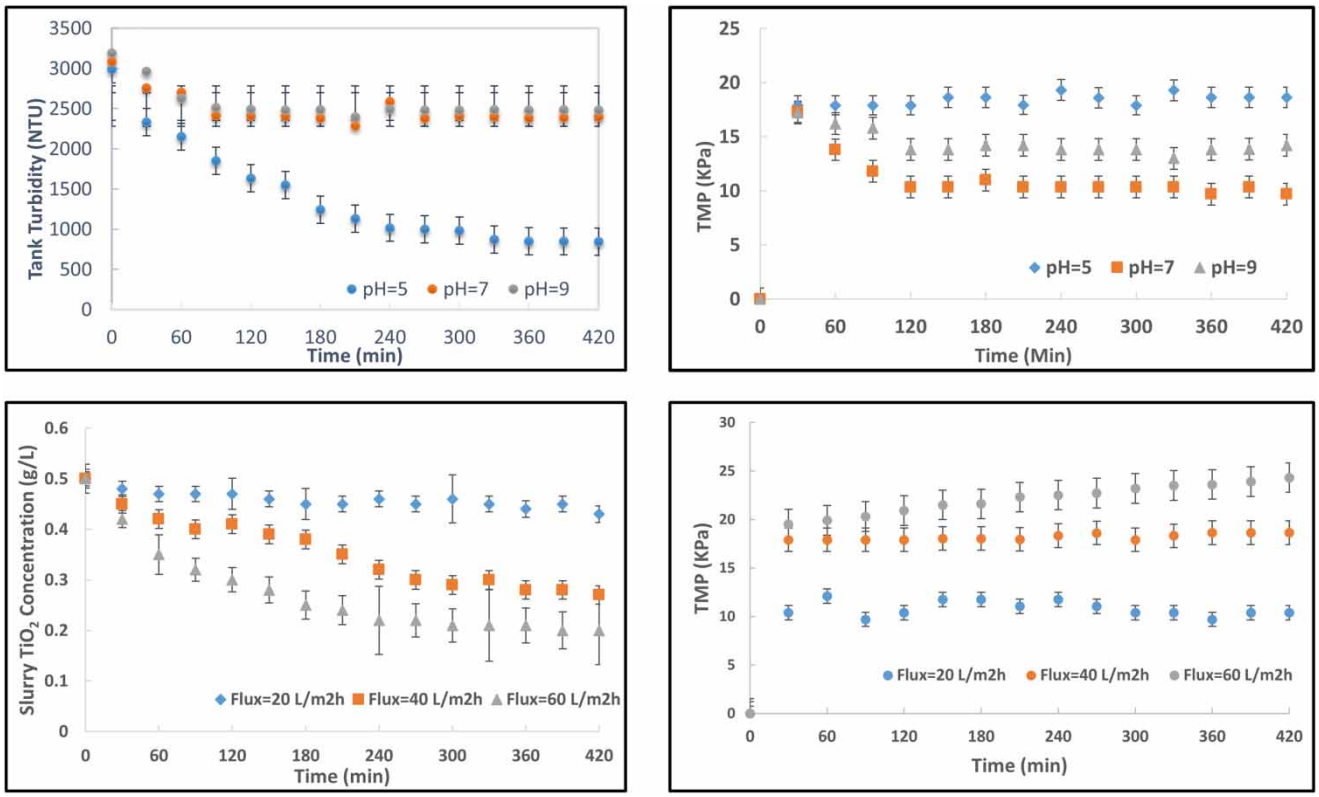

Figure 7 | Effect of pH – measured in terms of (a) tank turbidity and (b) TMP and effect of permeate flux – measured in terms of (c) slurry TiO_2 concentrations and (d) TMP on membrane fouling. The error bars denote standard deviation.

remained almost constant for hydrophobic PES membrane. This could be explained as the hydrophilic effect of TiO_2 which was dominated by the resistance offered by dense cake layer that resulted in no drop of TMP for hydrophobic PES membrane.

The pH of the reaction solution is an important parameter which influences the interaction between TiO_2 particles and the membrane (Damodar & Swaminathan 2008). It also affects the surface charges of TiO_2 photocatalyst.

$$pH > P_{zc}: TiOH + OH^- \rightarrow TiO^- + H_2O \quad (2)$$

$$pH < P_{zc}: TiOH + H^+ \rightarrow TiOH_2^+ \quad (3)$$

The reason for less fouling at $pH > 7$ may be due to the same negative charge on both the membrane and TiO_2. The surrounding turbulence might have removed the fouling layer at this pH condition. TiO_2 holds a positive charge at $pH < 6.8$ and negative charge at $pH > 6.8$, whereas membrane was negatively charged at $pH > 3$ (Damodar *et al.* 2012). However, at $pH = 5$, more TiO_2 particles were attracted towards the membrane surface since TiO_2 particles (positive charge) and membrane surface (negative charge) were oppositely charged and hence the fouling rate was accelerated. Therefore, at this pH condition, in order to remove TiO_2 particles on the membrane surface, the shear force needed was provided by means of aeration. However, while choosing the operating conditions for PMR, due consideration should be given to membrane fouling.

In general, there was less fouling when pH >7. This result was consistent with the report of others (Xi & Geissen 2001; Damodar *et al.* 2012; Zhang *et al.* 2013). Damodar *et al.* (2012) reported that at P_{zc}, the surface charge approaches zero leading to particle agglomeration and better fouling control (Erdei *et al.* 2008). Mendret *et al.* (2013) employed a composite TiO_2/Al_2O_3 membrane and noticed that the amount of fouling depended upon the zeta potentials of feed suspension particles and membrane surface. Wang *et al.* (2013) reported that the adjustment of pH decreases the contact angle of membrane and reduced the deposition of TiO_2 particles. In addition, the fractional dimension of TiO_2 aggregates also varied with pH, which resulted in the variation of amount and structure of cake layer. Zhang *et al.* (2013) reported that the TiO_2 aggregates were increased

at pH = 4.0 and pH = 6.0 due to dye-TiO_2 interaction and reduced at pH = 10. The fractional dimension of TiO_2 aggregates were decreased with pH, whereas pH = 10 exhibited higher flux decline and specific cake resistance. Therefore, alkaline conditions could improve photocatalytic degradation, avoid more adsorption and optimize the interaction between TiO_2 particles and the membrane.

Turbidity measurements were carried out before and after UF process to assess the extent of membrane fouling. The slurry TiO_2 concentrations were obtained from turbidity vs concentration calibration curve. The drop in feed and permeate turbidity indicate the amount of TiO_2 fouled on the membrane surface. In this study, from an initial turbidity of about 3,190 NTU (corresponding to a TiO_2 dose of 0.5 g/L), the permeate turbidities were dropped to <0.5 NTU. This result was in line with the results obtained by others (Sopajaree *et al.* 1999; Damodar *et al.* 2012; Szymański *et al.* 2016). Sopajaree *et al.* (1999) employed a polysulfone (PS) hollow fiber UF membrane (MWCO 100 KDa) and observed that the permeate turbidity during all the experiments were in the range of 0.22 NTU-0.42 NTU (TiO_2 dose of 1 g/dm^3) for an initial turbidity of 5,200 NTU. Damodar *et al.* (2012) utilized a MF PTFE (polytetrafluoroethylene) membrane of pore size 0.22 µm and noticed that the nano sized TiO_2 (TiO_2 dose of 0.5 g/L) were efficiently separated by the MF membrane. The permeate turbidity obtained during all the experiments were below 4 NTU indicates the remarkable separation properties of the membrane used. Another study carried out by Szymański *et al.* (2016) utilizing ceramic UF membrane for NOM removal revealed that the UF membrane was very much efficient in separating photocatalyst particles. The turbidity of permeate of 0.2 NTU obtained during all the experiments regardless of the process parameters applied confirmed the excellent separating performance of the membrane.

Effect of permeate flux on fouling

The effect of permeate flux measured in terms of slurry TiO_2 concentrations and TMP are shown in Figure 7(c) and (d), When the permeate flux increased from 20 to 60 L/m^2 h, increased amount of TiO_2 particles were accumulated on the membrane surface which in turn caused reduction in slurry TiO_2 concentration. This reduction in slurry TiO_2 concentration might have affected the degradation efficiency of the PMR. The TMP variation throughout the experiment was maintained constant. During experimentation it was also noticed that the TMP increased almost linearly with an increase in flux. Similar observations were made by others such as Choo *et al.* (2008) (hollow fiber membrane, flux = 15–100 L/m^2 h, pH = 7, humic acid concentration = 10 mg/L) and Damodar *et al.* (2012) (flat sheet membrane, flux = 32–64 L/m^2 h, pH = 5, [TiO_2] = 0.6 g/L).

The turbidity of the reaction mixture was tested under different flux conditions (31, 62, 93 mL/min i.e 20, 40, 60 L/m^2 h) and the results are shown in Figure 7(d). Severe fouling was observed at pH = 5 and less fouling occurred at pH ≥7. Fouling (TiO_2 deposition) was measured in terms of slurry TiO_2 concentrations and TMP. As the flux increases from 20 to 60 L/m^2 h, more TiO_2 particles were deposited on the membrane surface and, hence, reduction in slurry TiO_2 concentrations and TMP. At pH ≥7, increase in flux did not show much variation in fouling and TMP remained constant. Similar observations were made by others (Choo *et al.* 2008; Szymański *et al.* 2016). Choo *et al.* (2008) investigated the effect of flux 15–100 L/m^2 h on TMP variation. The higher the flux, the larger the suction pressure. Furthermore, the suction pressure at each flux (from 15 to 70 L/m^2 h) applied was maintained at a constant level during 250 min of PMR operation. In addition, a slight increase of pressure with time was observed at a flux of 100 L/m^2 h and indicated that almost no membrane fouling at fluxes >25 L/m^2 h in PMR. Szymański *et al.* (2016) reported that alkaline conditions (pH = 9) had a negative influence on the permeate flux, whereas at pH = 3 and pH = 6.5 no membrane fouling was observed.

CONCLUSIONS

A slurry PMR was evaluated for photocatalytic degradation of PHE and TOC removal during continuous experiments and the removal efficiencies were found to be 97% and 79%, respectively. The continuous operability and reusability studies performed in PMR revealed that TiO_2 could be efficiently reused. The major intermediates identified in this study were mainly quinones ketones and alcohols. Furthermore, the TiO_2 fouling on the membrane surface was confirmed by AFM, SEM and EDS studies. The average roughness of the membrane surface was found to increase from 1.131 nm to 28.041 nm. Membrane fouling was found to be profound when permeate flux was higher. Less fouling was observed during alkaline conditions. Therefore, while choosing the operating conditions for PMR, careful consideration should be given for membrane fouling. Meanwhile, alkaline conditions in the reactor was found to enhance photocatalytic degradation and reduce membrane fouling. In addition, the

studies revealed that the slurry PMRs could be operated efficiently with lower permeate fluxes.

ACKNOWLEDGEMENTS

The authors would like to acknowledge University Grants Commission (UGC), New Delhi, India for rendering financial support while carrying out this research work. The authors also would like to acknowledge Murugappa Chettiar Research Centre (MCRC), Taramani, India for granting access to TOC analysis.

CONFLICT OF INTEREST

The authors declare no conflict of interest.

REFERENCES

Abdel-Shafy, H. I. & Mansour, M. S. M. 2016 A review on polycyclic aromatic hydrocarbons: source, environmental impact, effect on human health and remediation. *Egyptian Journal of Petroleum* **25** (1), 107–123.

Adewuyi, Y. G. 2005 Sonochemistry in environmental remediation. 1. Combinative and hybrid sonophotochemical oxidation processes for the treatment of pollutants in water. *Environmental Science and Technology* **39** (10), 3409–3420.

Anandan, S., Vinu, A., Mori, T., Gokulakrishnan, N., Murugesan, V. & Ariga, K. 2007 Photocatalytic degradation of 2, 4, 6 - trichlorophenol using lanthanum doped ZnO in aqueous suspension. *Catalysis Communications* **8** (9), 1377–1382.

Baker, R. W. 2004 *Membrane Technology and Applications*, 2nd edn. Wiley, Chichester, UK.

Bavel, B. V. 2006 Comparison of Fenton's Reagent and ozone oxidation of polycyclic aromatic hydrocarbons in aged contaminated soils. *Journal of Soils and Sediments* **6** (4), 208–214.

Chong, M. N., Jin, B., Chow, C. W. K. & Saint, C. 2010 Recent developments in photocatalytic water treatment technology: a review. *Water Research* **44** (10), 2997–3027.

Choo, K. H., Chang, D. I., Park, K. W. & Kim, M. H. 2008 Use of an integrated photocatalysis/hollow fiber microfiltration system for the removal of trichloroethylene in water. *Journal of Hazardous Materials* **152** (1), 183–190.

Comninellis, A., Kapalka, A., Malato, S., Parsons, S. A., Poulios, I. & Mantzavinos, D. 2008 Advanced oxidation processes for water treatment: advances and trends for R&D. *Journal of Chemical Technology and Biotechnology* **83** (1), 769–776.

Damodar, R. A. & Swaminathan, T. 2008 Performance evaluation of a continuous flow immobilized rotating tube photocatalytic reactor (IRTPR) with TiO_2 catalyst for azo dye degradation. *Chemical Engineering Journal* **144** (1), 59–66.

Damodar, R. A. & You, S.-J. 2010 Performance of an integrated membrane photocatalytic reactor for the removal of Reactive Black 5. *Separation and Purification Technology* **71** (1), 44–49.

Damodar, R. A., You, S.-J. & Qu, S. H. 2010 Coupling of membrane separation with photocatalytic slurry reactor for advanced dye wastewater treatment. *Separation and Purification Technology* **76** (1), 64–71.

Damodar, R. A., You, S. J. & Chiou, G. W. 2012 Investigation on the conditions mitigating membrane fouling caused by TiO_2 deposition in a membrane photocatalytic reactor (MPR) used for dye wastewater treatment. *Journal of Hazardous Materials* **203–204**, 348–356.

Dewar, M. J. S. 1952 A molecular-orbital theory of organic chemistry. VI. Aromatic substitution and addition. *Journal of American Chemical Society* **74** (13), 3357–3363.

D'Souza, N. M. & Mawson, A. J. 2005 Membrane cleaning in the dairy industry: a review. *Critical Reviews in Food Science and Nutrition* **45** (2), 125–134.

Erdei, L., Arecrachakul, N. & Vigneswaran, S. 2008 A combined photocatalytic slurry reactor-immersed membrane module system for advanced wastewater treatment. *Separation and Purification Technology* **62** (2), 382–388.

Fernandez, R. L., McDonald, J. A., Khan, S. J. & Le-Clech, P. 2014 Removal of pharmaceuticals and endocrine disrupting chemicals by a submerged membrane photocatalysis reactor (MPR). *Separation and Purification Technolology* **127**, 131–139.

Freeman, D. J. & Cattell, F. C. R. 1990 Wood burning as a source of atmospheric polycyclic aromatic hydrocarbons. *Environmental Science and Technology* **24** (10), 1581–1585.

Harrison, R. M., Perry, R. & Wellings, R. A. 1976 Effect of water chlorination upon levels of some polynuclear aromatic hydrocarbons in water. *Environmental Science and Technology* **10** (12), 1151–1156.

Herrmann, J. H. 1999 Heterogeneous photocatalysis: fundamentals and applications to the removal of various types of aqueous pollutants. *Catalysis Today* **53** (1), 115–129.

Jiang, H., Zhang, G., Huang, T., Chen, J., Wang, Q. & Meng, Q. 2010 Photocatalytic membrane reactor for degradation of acid red B wastewater. *Chemical Engineering Journal* **156** (3), 571–577.

Kozak, K., Ruman, M., Kosek, K., Karasi, G., Stanchnik, L. & Polkowska, Z. 2017 Impact of volcanic eruptions on the occurrence of PAHs compounds in the aquatic ecosystem of the southern part of West Spitsbergen (Hornsund Fjord, Svabard). *Water* **9** (42), 1–21.

Laohaprapanon, S., Matahum, J., Tayo, L. & You, S. H. 2015 Photodegradation of Reactive black5 in a ZnO/UV slurry membrane reactor. *Journal Taiwan Institute of Chemical Engineers* **49** (1), 136–141.

Lin, H. F. & Valsaraj, K. T. 2003 A thin film annular photocatalytic reactor for the degradation of polycyclic aromatic hydrocarbons in dilute water streams. *Journal of Hazardous Materials* **B99**, 203–219.

Lloyd, D. 1989 *The Chemistry of Conjugated Cyclic Compounds: To be or not to be Like Benzene?* John Wiley, New York, NY, USA.

Mahamuni, N. N. & Adewuyi, Y. G. 2010 Advanced oxidation processes (AOPs) involving ultrasound for wastewater

treatment: a review with emphasis on cost estimation. *Ultrasonics Sonochemistry* **17** (6), 990–1003.

Mendret, J., Fraile, M., Rvallin, M. & Broillon, S. 2013 Hydrophilic composite membranes for simultaneous separation and photocatalytic degradation of organic pollutants. *Separation and Purification Technology* **111**, 9–19.

Moritz, T., Benfer, S., Arki, P. & Tomandl, G. 2001 Influence of the surface charge on the permeate flux in the dead-end filtration with ceramic membranes. *Separation and Purification Technology* **25** (1–3), 501–508.

Moursy, A. S. & Abdel-Shafy, H. I. 1983 Removal of hydrocarbons from Nile water. *Environment International* **9** (3), 165–171.

Mozia, S. 2010 Photocatalytic membrane reactors (PMRs) in water and wastewater treatment: a review. *Separation and Purification Technology* **73** (2), 71–91.

Mozia, S., Darowna, D., Orecki, A., Wrobel, R., Wilpiszewska, K. & Morawski, A. W. 2014 Microscopic studies on TiO_2 fouling of MF/UF polyether sulfone membranes in photocatalytic membrane reactor. *Journal of Membrane Science* **470** (2014), 356–368.

Muruganandham, M., Suri, R. P. S., Jafari, Sh., Sillanpaa, M., Lee, G. J., Wu, G. J., Wu, J. J. & Swaminathan, M. 2014 Recent Developments in homogeneous advanced oxidation processes for water and wastewater treatment. *International Journal of Photoenergy* **2014**, 1–24.

Nashio, J., Tokumura, M., Znad, H. T. & Kawase, Y. 2006 Photocatalytic decolourization of azo dye with zinc oxide powder in an external UV light irradiation slurry photoreactor. *Journal of Hazardous Materials* **138** (1), 106–115.

Paz, Y. 2006 Preferential photodegradation- why and how? *Comptes Rendus Chimie* **9** (5–6), 774–787.

Pereira, V. J., Weinberg, H. & Singer, P. 2004 Temporal and spatial variability of DBPs in a chlorinated distribution system. *Journal of American Water Works Association* **96**, 91–102.

Psillakis, E., Goula, G., Karlogerakis, N. & Mantzavinos, D. 2004 Degradation of polycyclic aromatic hydrocarbons in aqueous solutions by ultrasonic radiation. *Journal of Hazardous Materials* **B108**, 95–102.

Qu, D., Qiang, Z., Xiao, S., Liu, Q., Lei, Y. & Zhou, T. 2014 Degradation of reactive black 5 in a submerged photocatalytic reactor with microwave electrodeless lamps as light source. *Separation and Purification Technology* **122**, 54–59.

Rahimpour, A., Jahanshahi, M., Rajaeian, B. & Rahimnejad, M. 2011 TiO_2 entrapped nano-composite PVDF/SPES membranes: Preparation, characterization, antifouling and antibacterial properties. *Desalination* **278**, 343–353.

Rani, C. N. & Karthikeyan, S. 2016 Endocrine disrupting compounds in water and wastewater and their treatment options – a review. *International Journal of Environmental Technology and Management* **19** (5/6), 392–431.

Sarasidis, V. C., Plakas, K. V., Patsios, S. I. & Karabelas, A. J. 2014 Investigation of diclofenac degradation in a continuous photocatalytic membrane reactor. Influence of operating parameters. *Chemical Engineering Journal* **239**, 299–311.

Sofia, J., Yiva, P., Sofia, F. & Staffan, L. 2006 Comparison of Fenton's reagent and ozone oxidation of polycyclic aromatic hydrocarbons in aged contaminated soils. *Journal of Solids and Sediments* **6** (4), 208–214.

Sopajaree, K., Qasim, S. A., Basak, S. & Rajeshwar, K. 1999 An integrated flow reactor-membrane filtration system for heterogeneous photocatalysis. Part II: Experiments on the ultrafiltration unit and combined operation. *Journal of Applied Electrochemistry* **29** (9), 1111–1118.

Szymański, K., Morawski, A. W. & Mozia, S. 2016 Humic acids removal in a photocatalytic membrane reactor with ceramic UF membrane. *Chemical Engineering Journal* **305**, 19–27.

Vela, N., Martinez-Menchon, M., Navarro, G., Parez-Lucas, G. & Navarro, S. 2012 Removal of polycyclic aromatic hydrocarbons (PAHs) from ground water by heterogeneous photocatalysis under natural sunlight. *Journal of Photochemistry and Photobiology A: Chemistry* **232**, 32–40.

Wang, R., Ren, D., Xia, S., Zhang, Y. & Zhao, J., 2009 Photocatalytic degradation of Bisphenol A (BPA) using immobilized TiO_2 and UV illumination in a horizontal circulating bed photocatalytic reactor (HCBPR). *Journal of Hazardous Materials* **169** (1–3), 926–932.

Wang, P., Fane, A. G. & Lim, T. T. 2013 Evaluation of a submerged membrane vis-LED photoreactor (SMPR) for carbamazepine degradation and TiO_2 separation. *Chemical Engineering Journal* **215–216**, 240–251.

Wen, S., Zhao, J., Sheng, G., Fu, J. & Peng, P. 2002 Photocatalytic reactions of phenanthrene at TiO_2 interfaces. *Chemosphere* **46** (6), 871–877.

Woo, O. T., Chung, W. K., Wong, K. H., Chow, A. T. & Wong, P. K. 2009 Photocatalytic oxidation of polycyclic aromatic hydrocarbons: intermediates identification and toxicity testing. *Journal of Hazardous Materials* **168** (2–3), 1192–1199.

Xi, W. & Geissen, S.-U. 2001 Separation of titanium dioxide from photocatalytically treated water by cross-flow microfiltration. *Water Research* **35** (5), 1256–1262.

Xiao, Y., Tong, F., Kuang, Y. & Chen, B. 2014 Distribution and source appointment of polycyclic aromatic hydrocarbons (PAHs) in forest soils from urban to rural areas in the Pearl River delta of southern China. *International Journal of Research and Public Health* **11** (3), 2642–2656.

Zeng, Y., Hong, A. P. K. & Wavrek, D. A. 2000 Chemical-biological treatment of pyrene. *Water Research* **34** (4), 1157–1172.

Zhang, G., Zhang, J., Wang, L., Meng, Q. & Wang, J. 2012 Fouling mechanism of low-pressure hollow fibre membranes used in separating nanosized photocatalysts. *Journal of Membrane Science* **389**, 532–543.

Zhang, J., Wang, L., Wang, L., Zhang, G., Wang, Z., Xu, L. & Fan, Z. 2013 Influence of azo dye-TiO_2 interactions on the filtration performance in a hybrid photocatalysis/ultrafiltration process. *Journal of Colloid and Interface Science* **389** (1), 273–283.

Zhang, W., Luo, J., Ding, L. & Jaffrin, M. Y. 2015 A review on flux decline control strategies in pressure-driven membrane processes. *Industrial and Engineering Chemistry Research* **54** (11), 2843–2861.

First received 14 August 2017; accepted in revised form 4 May 2018. Available online 15 May 2018